GEOPHYSICAL RESEARCH LETTERS, VOL. 8, NO. 8, PAGES 887-890, AUGUST 1981

FRACTURE ENERGY OF STICK-SLIP EVENTS IN A LARGE SCALE BIAXIAL EXPERIMENT

Paul G. Okubo and James H. Dieterich

Branch of Tectonophysics, U.S. Geological Survey, Menlo Park, California 94025

Abstract. The concept of apparent fracture energy for the shear failure process is employed by many authors in modeling earthquake sources as dynamically extending shear cracks. Using records of shear strain and relative displacement from stick-slip events generated along a simulated, prepared fault surface in a large (1.5m x 1.5m x 0.4m) granite block and a slip-weakening model for the fault, direct estimates of the apparent shear fracture energy of the stick-slip events have been obtained. For events generated on a finely ground fault surface, apparent fracture energy ranges from 0.06 J/m^2 at a normal stress of 1.1 MPa to 0.8 J/m^2 at a normal stress of 4.6 MPa. In contrast to estimates for tensile crack formation, we find that the apparent fracture energy of stick-slip events increases linearly with normal stress. The results for the slip-weakening model for the stick-slip events are generally consistent with constitutive fault models suggested by observations of stable sliding in smaller scale experiments.

Introduction

A fundamental parameter for modeling earthquakes as dynamically extending shear cracks is the energy required to create newly faulted surface area, or the apparent fracture energy. A failure criterion or equation of motion for the advancing crack can be formulated in which the crack advances if the energy available to the region surrounding the crack tip due to the applied loads equals the fracture energy. Estimates of earthquake fracture energy derived from theoretical studies range from 1 J/m^2 to 10^8 J/m^2 (Ida, 1973; Husseini, et al., 1975 and 1976; Aki, 1979). Husseini, et al. associate the lower end of this range, from 1 J/m^2 to 10^4 J/m^2, with frictional failure and the upper end, from 10^4 J/m^2, with fresh fracture.

There is little published experimental work from which direct estimates of apparent fracture energy of shear failures can be made. Laboratory estimates of tensile fracture energy, or surface energy, of minerals range between 1 J/m^2 and 10 J/m^2 (Brace and Walsh, 1962). Surface energies of a variety of rock types are on the order of 10 J/m^2 (Friedman, et al., 1972). Many authors refer to these values while discussing earthquake fracture energy, but, although surface energy might be a significant component of the apparent fracture energy of faulting, the relationship is not yet clearly established.

Here we present some laboratory estimates of the apparent shear fracture energy of stick-slip events generated on a prepared fault surface in a large rock sample. We also attempt to infer the way in which physical properties of the fault and experimental conditions control apparent shear fracture energy.

Data

The data presented here are obtained from experiments performed in a large scale biaxial testing machine. Dieterich, et al. (1978) discuss details of the apparatus. The sample is a 150 cm x 150 cm x 40 cm block of Sierra white granite from the Raymond, California, quarry. A fault is simulated in the sample by a finely ground sawcut oriented at an angle of 45° to the sides of the block. The fault has a measured roughness of 0.2 microns. Two independently controlled sets of hydraulic flatjacks apply loads to the sample. Stick-slip events are generated on the fault by gradually increasing the shear stress on the fault using manually operated flow valves.

The experiments summarized here are carried out at a number of different normal stress levels between 1 MPa and 5 MPa. The shear stress is increased at a rate of approximately 3×10^{-4} MPa/second. A network of semiconductor strain gages is mounted along the fault to monitor the component of shear strain parallel to the fault. Velocity transducers are co-located with the strain gages to monitor relative slip between the two sides of the fault. The strain gage outputs have been calibrated against the pressure transducer records and are scaled to give local shear stress as a function of time. The velocity transducers are calibrated against sensitive high-frequency displacement transducers as well as LVDT instruments which accurately record the static fault offsets.

Figure 1 shows an example of the high-speed recordings from a stick-slip event that was generated at a normal stress of $\sigma = 1.9$ MPa. The signals from the strain gages and velocity transducers at five different locations along the fault are recorded digitally at a rate of 200,000 samples/second. The high-frequency oscillations in the velocity records are due, at least in part, to resonances in the transducers excited during the stick-slip event. The velocity records are also integrated once in the time domain to provide records of fault slip.

Several interesting features of the stick-slip failure of the fault are seen in records like those shown in Figure 1. (i) Slip along the fault associated with the stick-slip event begins with a rapid decrease in shear stress. Sliding continues at a lower, relatively constant residual shear stress level until the end of the event. (ii) Slip is preceded over fractions of a millisecond by gradual increases in shear stress along the fault resulting from cohesive or other processes which initially resist the onset of slip. (iii) The stress drops at different locations on the fault do not occur simultaneously. Instead, they occur at different

Paper number 1L1073.

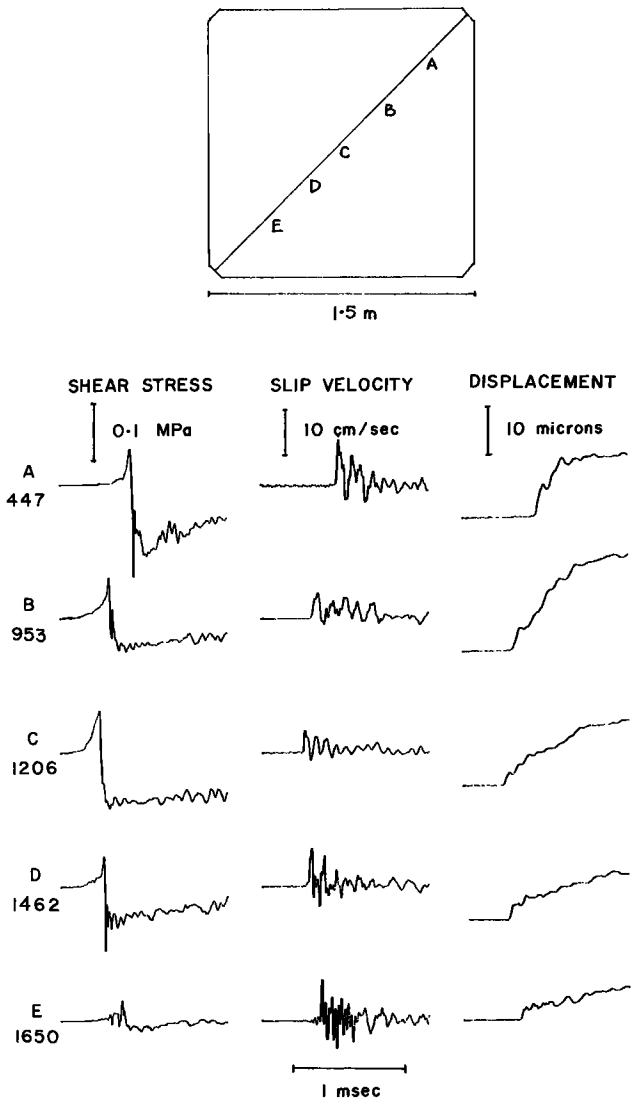

Figure 1. Data from stick-slip event generated at σ = 1.9 MPa. Numbers along left side of figure indicate distances in mm measured from upper right-hand corner of block to transducers. Vertical and horizontal scales as shown.

times, indicating propagation of the stick-slip failure from a nucleation point to other locations on the fault. In Figure 1, the event begins near the center of the fault and the failure propagates bilaterally at an apparent rupture velocity of about 2-1/2 km/second. (iv) The stress drops, while rapid, do occur over finite time intervals. During this time as the fault weakens, the fault slips a finite amount. We refer to such behavior as slip weakening of the fault, and we discuss this idea below.

The strain gages and velocity transducers provide records of the local shear stress and local fault slip. Figure 2a gives examples of point-by-point plots of stress against displacement. The drops from peak shear stress to residual shear stress are not achieved until a finite displacement, in this case about 2-1/2 microns, is reached. Such slip weakening behavior of the fault is similar to that observed in quasi-static sliding experiments using small laboratory samples (Dieterich, 1978 and 1980).

Analysis

Ida (1972), Palmer and Rice (1973), Andrews (1976), and Freund (1979) discuss slip weakening models in the contexts of shear crack propagation and other shear failure processes. These models for shear failures may be viewed as extensions of cohesive force models for tensile cracks developed by Barenblatt (1962) and others. Figure 2b illustrates idealized slip weakening as observed in these experiments. Local stress on the fault increases from an initial value τ_o due to processes which resist the onset of slip. When the shear stress reaches a peak value τ_p, slip begins. Initially, stress decreases linearly with displacement until a critical displacement, d_r, is reached. Beyond the critical displacement, the stress required to sustain further sliding is the constant residual value τ_r.

For this model, apparent fracture energy is the energy required to overcome the cohesive forces and advance the rupture along the fault. Equivalently, it is the work done during faulting in excess of that work which is required to overcome the effects of dynamic friction (the shaded area in Figure 2b). Note that with this model, the apparent fracture energy depends explicitly on the stress drop ($\tau_p - \tau_r$) accompanying the failure and the critical displacement d_r. The apparent fracture energy is also referred to as the cohesive energy density of the fault (Freund, 1979) and, under certain conditions, the energy release rate of faulting (e.g., Rice, 1979).

Figures 3, 4, and 5 summarize the results from fifteen stick-slip events. From stress-

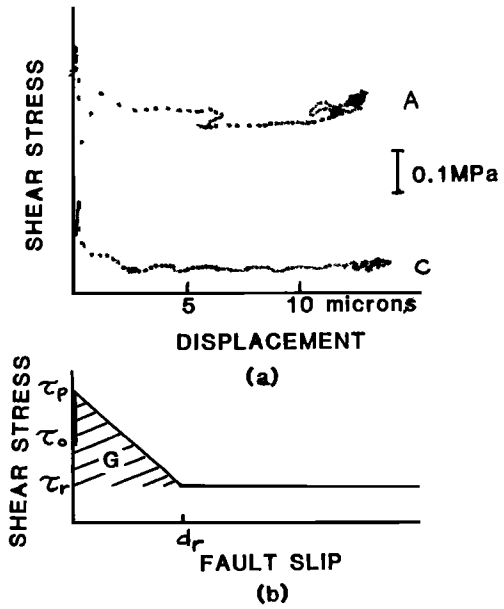

Figure 2. Slip-weakening curves. (a) Observed slip-weakening at two locations for stick-slip event shown in Figure 1. (b) Slip-weakening model with linear decrease in shear stress with slip. Shaded area represents apparent shear fracture energy.

vs-displacement plots like Figure 2a, we estimate d_r and the peak to residual shear stress drop. By approximating the observed slip weakening of the fault with the simple slip weakening model shown in Figure 2b, we finally estimate the apparent fracture energy of the events.

Critical displacements d_r at the individual transducer locations are plotted against normal stress in Figure 3. There is a clustering of d_r values between 2 and 3 microns for all values of normal stress. The mean value is $d_r = 2.8 \pm 1.8$ (s.d.) microns. The scattering of points giving large values of d_r generally come from complicated records which suggest closely stacked double or multiple stick-slip events during a single experiment. The critical displacement value of $d_r = 2.8$ microns, insensitive to normal stress, is consistent with quasi-static results for a finely ground surface with no gouge present (Dieterich, 1980).

Averages of local stress drops $(\tau_p - \tau_r)$ for each event are plotted against normal stress in Figure 4. Consistent with other laboratory stick-slip observations, e.g., Scholz et al. (1972), stress drop increases with normal stress. Average stress drops increase linearly with normal stress with a proportionality constant of 0.1, over the range of normal stresses used here.

Taking the definition of apparent fracture energy G from the slip weakening model that we have used and the observations that: (i) critical displacement is independent of normal stress and (ii) stress drop increases linearly with normal stress, we would expect the apparent shear fracture energy of these events also to increase linearly with normal stress. Figure 5 plots the average apparent fracture energy for each event obtained from individual slip weakening curves. The result roughly agrees with our prediction: the average apparent shear fracture energy of the stick-slip events increases approximately linearly with normal stress. It is important to note the observed linear dependence of apparent shear fracture energy on normal stress. This differs markedly from observations made of tensile fracture energy or surface energy which is generally regarded as a material property and, as such, shows no similar dependence on normal stress.

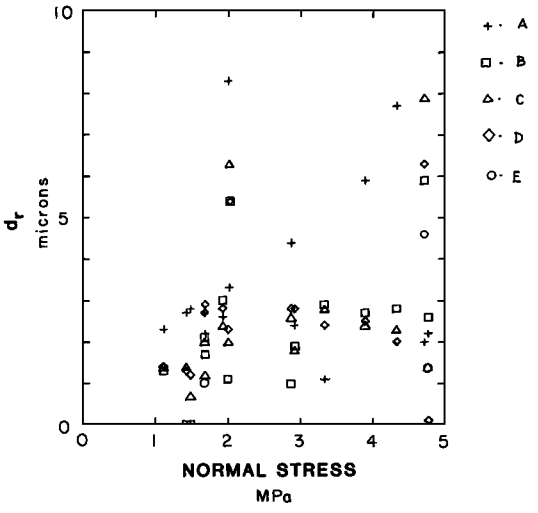

Figure 3. Critical displacements d_r measured at different transducer locations along fault plotted against normal stress.

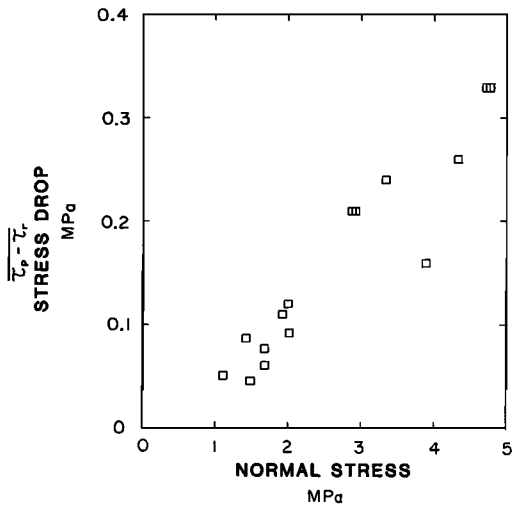

Figure 4. Average stress drops of stick-slip events plotted against normal stress.

Discussion and Summary

We can summarize the results of detailed observations of stick-slip failures on a prepared fault surface as follows: (i) At the beginning of stick-slip, displacement weakening of the fault occurs. The critical displacement, d_r, associated with the slip weakening is independent of the normal stress at which the event is generated. It is also interesting to note that the observed slip weakening is similar in appearance to the hypothetical slip weakening model chosen by Andrews (1976) to numerically model dynamic shear cracks. (ii) The dynamic stress drops of the events increase linearly with normal stress. (iii) The apparent shear fracture energy G of the events increases linearly with normal stress.

Rice (1979) presents an analysis of results of Rummel, et al. (1978) of tests on polished sawcut surfaces under 470 MPa confining pressure from which he obtains an estimate of G equal to 4.5×10^4 J/m^2. This exceeds the range suggested by Husseini, et al. (1975 and 1976) for frictional failures. A direct extrapolation of our results to that level of normal stress yields a G of 60 J/m^2. The origin of this apparent discrepancy between estimates of G for polished surfaces is not clear, but it may lie in the remote measurements of displacement and load parameters in Rummel's tests or the presumably greater amount of surface damage suffered under high normal stresses.

For the slip weakening model that we have used, the critical displacement d_r is also important in controlling the size of G. Although the results presented here reveal no obvious factors that control d_r, results from smaller scale quasi-static friction experiments indicate that d_r depends on the physical properties of the fault surface (Dieterich, 1980), particularly fault roughness and the nature of fault gouge. Larger values for d_r arise when gouge is

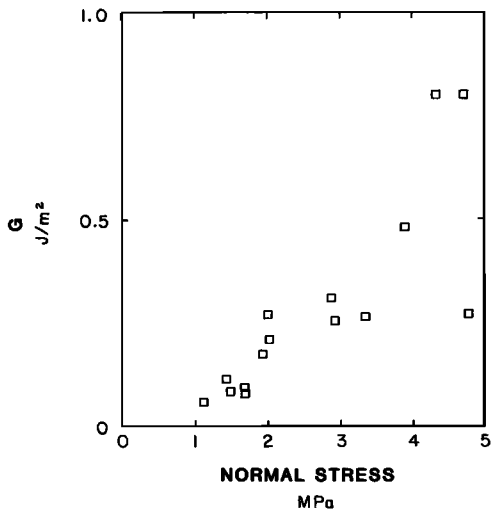

Figure 5. Average apparent fracture energy of stick-slip events plotted against normal stress.

present. The magnitude of d_r further increases with the roughness of the fault surfaces and the coarseness of the gouge. As seen in Dieterich (1980), even within the range of fault conditions readily tested in the laboratory, d_r can vary over two orders of magnitude. This implies that apparent fracture energy can also vary by a similar amount. If a natural fault is at least as rough as the most roughly ground simulated fault and contains coarse fault gouge, then we might expect that apparent fracture energy values for shear failures on natural faults would be at least two orders of magnitude greater than the values we have estimated here. In addition, if there exist variations in physical properties along a fault, then we might expect corresponding variations in G. Such variations in apparent fracture energy could act as barriers along the fault plane, as suggested by Das and Aki (1977), for example, and could affect processes associated with faulting, including the generation of strong ground motion during an earthquake.

References

Aki, K., Characterization of barriers on an earthquake fault, J. Geophys. Res., 84, 6140-6148, 1979.

Andrews, D. J., Rupture propagation with finite stress in antiplane strain, J. Geophys. Res., 81, 3575-3582, 1976.

Barenblatt, G. I., Mathematical theory of equilibrium cracks in brittle fracture, Adv. Appl. Mech., 7, 55-129, 1962.

Brace, W. F., and J. B. Walsh, Some direct measurements of the surface energy of quartz and orthoclase, Amer. Mineral., 47, 111-112, 1962.

Das, S., and K. Aki, Fault plane with barriers: A versatile earthquake model, J. Geophys. Res., 82, 5658-5670, 1977.

Dieterich, J. H., Time-dependent friction and the mechanics of stick-slip, Pure Appl. Geophys., 116, 790-806, 1978.

Dieterich, J. H., Constitutive properties of faults with simulated gouge, in press, 1980.

Dieterich, J. H., D. W. Barber, G. Conrad, and Q. A. Gorton, Preseismic slip in a large scale friction experiment, Proc. 19th U.S. Rock Mech. Symp., 110-117, 1978.

Freund, L. B., The mechanics of dynamic shear crack propagation, J. Geophys.Res., 84, 2199-2209, 1979.

Friedman, M., J. Handin, and G. Alani, Fracture-surface energy of rocks, Int. J. Rock Mech. Min. Sci., 9, 757-766, 1972.

Husseini, M. I., D. B. Jovanovich, M. J. Randall, and L. B. Freund, The fracture energy of earthquakes, Geophys.J.Roy.Astron.Soc., 43, 367-385, 1975.

Husseini, M. I., D. B. Jovanovich, and M. J. Randall, Fracture energy and aftershocks, Geophys.J.Roy.Astron.Soc., 45, 393-406, 1976.

Ida, Y., Cohesive force across the tip of a longitudinal shear crack and Griffith's specific surface energy, J.Geophys. Res., 77, 3796-3805, 1972.

Ida, Y., The maximum acceleration of seismic ground motion, Bull. Seismol. Soc. Am., 63, 959-968, 1973.

Palmer, A. C., and J. R. Rice, The growth of slip surfaces in the progressive failure of over-consolidated clay, Proc. Roy. Soc. London, Ser. A, 332, 527-548, 1973.

Rice, J. R., The mechanics of earthquake rupture, in Proceedings of the International School of Physics, "Enrico Fermi," Italian Physical Society, Course LXXVIII on Physics of the Earth's Interior, ed. by E. Boschi, North-Holland, Amsterdam, in press, 1979.

Rummel, F., H.J. Alheid, and C. Frohn, Dilatancy and fracture induced velocity changes in rock and their relation to frictional sliding, Pure Appl. Geophys., 116, 743-764, 1978.

Scholz, C. H., P. Molnar, and T. Johnson, Detailed studies of frictional sliding of granite and implications for the earthquake mechanism, J.Geophys.Res., 77, 6392-6406, 1972.

(Received May 20, 1981;
accepted June 23, 1981.)